

# Turbulent scaling law in Ogata Kōrin's *Red and White Plum Blossoms*

Takeshi Matsumoto<sup>1</sup>

*Division of Physics and Astronomy, Graduate School of Science, Kyoto University  
Kitashiarakawa Oiwakecho Sakyo-ku Kyoto, 606-8502, Japan.*

(\*Electronic mail: takeshi@kyoryu.scphys.kyoto-u.ac.jp)

(Dated: 20 January 2025)

Stylized turbulent swirls depicted in artworks are often analyzed with the modern tools for real turbulent flows such as the power spectrum and the structure function. Motivated by the recent study on *The Starry Night* of van Gogh (Ma *et al.*, Phys. Fluids, **36** 095140, 2024), we here analyze the swirling motif in Ogata Kōrin's *Red and White Plum Blossoms*. The results show that Kōrin's swirls follow closely the Obukhov–Corrsin spectrum  $k^{-5/3}$  in the inertial-convective range of the passive scalar advected by the homogeneous and isotropic turbulence. Furthermore the swirl's 4-th and 6-th structure functions exhibit approximately the same intermittent scaling law of the passive scalar.

## I. INTRODUCTION

Great artworks depicting fluid flows compel some fluid dynamicists to analyze them as they do for real flows in laboratory experiments, field measurements, and numerical simulations. Irresistible examples include Leonardo da Vinci's drawings<sup>1–3</sup>, *The Great Wave off Kanagawa* by Katsushika Hokusai<sup>4,5</sup>, and *The Starry Night* by van Gogh<sup>6–9</sup>, just to name a few.

Da Vinci's most celebrated drawing of turbulence *Studies of Water*, which depicts water from a duct falling into a larger pool and causing many air bubbles, is now numerically reproduced with the smoothed particle hydrodynamics method<sup>1,3</sup>. What is remarkable is that the attentions are drawn not only to realistic expressions of flows, but also to stylized ones, such as the works by Hokusai and van Gogh. *The Great Wave off Kanagawa* is compared with a photograph of a certain type of oceanic breaking waves taken from a research vessel, showing consistency of his distinctive expression with the physics<sup>5</sup>.

*The Starry Night* is well-known for the magnificent swirls in the sky at night. Those stylized swirls have been analyzed by calculating the power spectrum density of the luminance of the image<sup>7–9</sup>. It is considered that the luminance corresponds to the passive scalar advected by the real turbulent flow<sup>6,9</sup>. Indeed early studies find power-law scaling in the luminance spectrum. However its scaling exponent is a matter of debate<sup>7–9</sup>. A recent detailed study<sup>9</sup> shows that the luminance spectrum of the swirls is composed of  $k^{-5/3}$  and  $k^{-1}$  parts, where  $k$  is the wavenumber. They argue that the first and second parts correspond to the Obukhov–Corrsin spectrum and the Batchelor spectrum of the passive scalar turbulence at high Schmidt numbers<sup>9</sup>. The Batchelor-spectrum part is confirmed also by the second-order structure function of the luminance<sup>9</sup>. Therefore, the iconic swirls in *The Starry Night* respect the physical law of turbulent flows.

Motivated by this recent study<sup>9</sup>, we here analyze stylized turbulent swirls in a Japanese painting in the 18th century utilizing the spectrum and structure function. The painting is *Red and White Plum Blossoms* by Ogata Kōrin (1658–1716), which is shown in Fig. 1. It is less known than *The Great Wave off Kanagawa* by Hokusai (1760–1849). Nonetheless, *Red and White Plum Blossoms* is considered also as one of the most important Japanese artworks of the Edo period (1603–

1868). The artists influenced by the style of Kōrin and his predecessors are now called “Rin-pa”<sup>10</sup> coined from his given name. It is known that Hokusai is one of them (see e.g., Refs. 11 and 12).

Although the title *Red and White Plum Blossoms* does not mention it, the river is flowing between the red plum tree on the right and the white plum tree on the left. The flow is expressed by boldly stylized swirls that exhibit an irregular hierarchical structure. This intriguing hierarchy leads us to identify its scaling law. In particular, we first show that the luminance spectrum follows closely  $k^{-5/3}$ , which can be interpreted as the Obukhov–Corrsin spectrum<sup>13–15</sup> of the passive scalar advected by the homogeneous and isotropic turbulence. Then we demonstrate that the luminance obeys approximately the same intermittent scaling law of the passive scalar turbulence<sup>16–19</sup> by calculating the 4-th and 6-th order structure functions. Namely, the power-law exponents of the  $p$ -th order structure functions of the luminance in the scaling range are different from  $p/3$  ( $p = 4$  and  $6$  here), but approximately the same as those of the passive scalar. To the best of our knowledge, such consistency of an artwork with the real turbulent flow including the intermittency is not known.

Why is the stylized flow in *Red and White Plum Blossoms* created about 300 years ago quantitatively consistent with the detailed laws of the present-day fluid dynamics? Although we do not have an answer to this question yet, we will discuss about this point at the end of this paper together with the insights<sup>5,9</sup> obtained from *The Great Wave off Kanagawa* and *The Starry Night*.

The organization of the paper is as follows. In Sec.II we explain how we pre-process the electronic image of the painting. In Sec.III we analyze the luminance spectrum of the swirls. In Sec.IV we calculate the structure function of the luminance. Concluding discussions are given in Sec.V.

## II. PRE-PROCESS OF THE IMAGE DATA

We first convert the color JPG image of *Red and White Plum Blossoms* shown in Fig. 1 to a gray-scale image. We use the conversion formula,

$$Y = 0.2125R + 0.7154G + 0.0721B, \quad (1)$$



FIG. 1. Ogata Kōrin's *Red and White Plum Blossoms*, a collection of the MOA Museum of Art in Atami, Japan. This is a folding screen consisting of two separate panels. The black column in the center of this image is a margin between the two panels. The dimension of each panel is 156cm (height)  $\times$  172.2cm (width). The panels can be folded in the middle. This particular image (JPG format) provided by Google Art & Culture is available at Wikimedia Commons ([https://commons.wikimedia.org/wiki/File:Ogata\\_Kōrin\\_-\\_RED\\_AND\\_WHITE\\_PLUM\\_BLOSSOMS\\_\(National\\_Treasure\)\\_-\\_Google\\_Art\\_Pro](https://commons.wikimedia.org/wiki/File:Ogata_Kōrin_-_RED_AND_WHITE_PLUM_BLOSSOMS_(National_Treasure)_-_Google_Art_Pro)). The number of pixels of this image are  $4001 \times 1757$ , which is the largest available in the above URL.

from the red ( $R$ ), blue ( $B$ ) and green ( $G$ ) channels of the image to the gray scale ( $Y$ ). Those  $Y, R, G$  and  $B$  are defined on each pixel at  $(x, y)$ . The channel values are obtained here by using `cv2.split` of the library OpenCV (version 4.6.0) for computer vision with Python (version 3.12.8). The weight coefficients in Eq. (1) are the standard ones known as ITU Recommendation BT.709-6, or Rec.709, for high definition television<sup>20</sup>. The conversion method is the same as Ref. 9, but our coefficient values are slightly different from theirs. We check that the equal weights do not change the main results of this paper. The value  $Y(x, y)$  on each pixel is then transformed to a 8-bit integer value which lies between 0 to 255. Let us now define the luminance  $\theta(x, y)$  by

$$\theta(x, y) = \frac{\lfloor Y(x, y) \rfloor_8}{255}. \quad (2)$$

Here  $\lfloor \cdot \rfloor_8$  means the transformation to a 8-bit integer. The resultant luminance is shown in Fig. 2. We compare the field  $\theta(x, y)$  with the passive-scalar quantity advected by the homogeneous and isotropic turbulence (HIT), as proposed in Ref. 9 for *The Starry Night*.

We use mainly the pixel coordinates in the following spectral and structure function analysis. A pixel of the image shown in Fig. 1, or equivalently Fig. 2, can be regarded as a square by the following estimates. The height of a pixel can be estimated as  $156 \text{ [cm]} / 1756 \text{ [pixel]} \simeq 0.08884 \text{ [cm/pixel]}$ . We identify that the left-panel image extends horizontally from 0 to 1945 pixel and the right-panel image from 2062 to 4000 pixel. The width of a pixel can be estimated as  $172.2 \text{ cm} / 1945 \text{ [pixel]} \simeq 0.08853 \text{ [cm/pixel]}$  for the left panel and as  $172.2 \text{ cm} / 1938 \text{ [pixel]} \simeq 0.08885 \text{ [cm/pixel]}$  for the right panel.

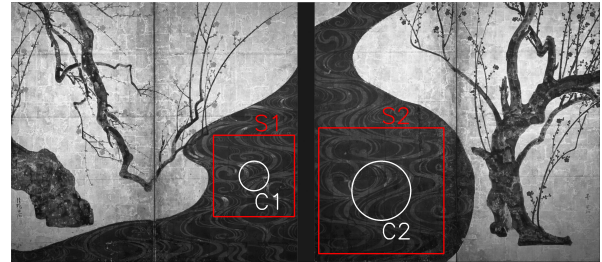


FIG. 2. Gray-scaled image of Fig. 1. More specifically, the luminance  $\theta(x, y)$  defined in Eq. (2). The annotated circular regions, C1 and C2, are used in the spectral analysis in Sec.III. The radii of C1 and C2 shown here are set to  $\sigma$ 's listed in Table I. The square regions, S1 and S2, are used in the structure-function analysis in Sec.IV.

### III. SPECTRUM VIA WINDOWED FOURIER TRANSFORM

Let us calculate the spectrum of  $\theta(x, y)$  in the river flowing between the white and red plum trees. Since we focus only on the river part of the painting, we adopt the windowed Fourier transform, also known as the Gabor transform. We consider two regions for calculating the spectrum. One of them is taken in the left panel as depicted C1 in Fig. 2 and the other one is taken in the right panel as depicted C2 in the same figure. The windowing is done with a two-dimensional Gaussian function,

$$\theta_w(x, y) = \theta(x, y) \frac{1}{2\pi\sigma^2} \exp\left[-\frac{|\mathbf{x} - \mathbf{x}_c|^2}{2\sigma^2}\right]. \quad (3)$$

The parameter values for C1 and C2 are listed in Table I. The windowed luminance field  $\theta_w(x, y)$  for the two regions are

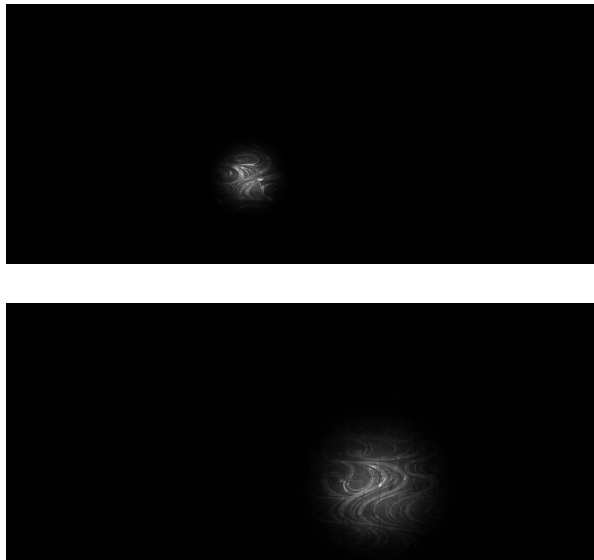


FIG. 3. Gaussian-windowed gray scale images for calculating the spectrum. The top and bottom panels correspond respectively to C1 and C2 in Fig. 2. The black color represents zero luminance after multiplied by the Gaussian function. The non-zero luminance (gray or white) in this figure is enhanced than that of Fig. 2 to highlight the effect of the windowing.

shown in Fig. 3. Indeed they include only the river regions.

The windowed field is then Fourier-transformed and the spectrum is calculated in a standard manner,

$$E_{\theta}(k) = \sum_{k \leq |\mathbf{k}| < k + \Delta k} \frac{1}{2} |\hat{\theta}_w(\mathbf{k})|^2 \frac{1}{\Delta k}. \quad (4)$$

Here  $\hat{\theta}_w(\mathbf{k})$  is the Fourier coefficient of the windowed luminance and  $\mathbf{k}$  is the wavevector. We take  $\Delta k = 2\pi/(4 \text{ [pixel]})$ .

The resultant spectra for C1 and C2 are plotted in Fig. 4. We observe the power-law behavior in the intermediate wavenumber range for both cases. This power law is consistent with the Obukhov–Corrsin (OC) spectrum,  $C\chi\varepsilon^{-1/3}k^{-5/3}$ , in the inertial-convective range for the passive scalar advected by HIT<sup>13–15</sup>. Here  $C$ ,  $\chi$ , and  $\varepsilon$  are the non-dimensional Obukhov–Corrsin constant, the scalar dissipation rate, and the energy dissipation rate, respectively.

This  $k^{-5/3}$  like power-law part of the luminance spectrum is followed by the steeply decreasing part in the larger wavenumbers. This is in contrast to the spectrum found in *The Starry Night* where the  $k^{-5/3}$  part is followed by the shallower Batchelor spectrum  $k^{-1}$  of the dissipative-convective range<sup>9</sup>. Our decreasing part for  $k \geq 1 \text{ [(pixel)}^{-1}]$  in Fig. 4 may correspond to the dissipation-range behavior (non power-law behavior) of the passive scalar spectrum. Or it may correspond to the Batchelor–Howells–Townsend spectrum,  $\tilde{C}\chi\kappa^{-3}\varepsilon^{2/3}k^{-17/3}$ , of the passive scalar at low Schmidt numbers in the inertial-diffusive range<sup>21</sup>, as indicated in Fig. 4 by the dashed line. Here  $\tilde{C}$  and  $\kappa$  are the non-dimensional constant and the diffusivity of the passive scalar, respectively. The two possibilities suggest that the luminance is analogous

TABLE I. Parameters of the Gaussian window. The center coordinates  $\mathbf{x}_c$  and the width  $\sigma$  are given in terms of pixels of Fig. 1. Notice that the  $y$  coordinate is increasing from top to bottom. The coordinate origin  $\mathbf{x} = (0, 0)$  is the left-top corner of the figure. The coordinates of the right-bottom corner is (4000, 1756).

Region	$\mathbf{x}_c$ [pixels]	$\sigma$ [pixels]
C1	(1650, 1175)	100
C2	(2515, 1275)	200

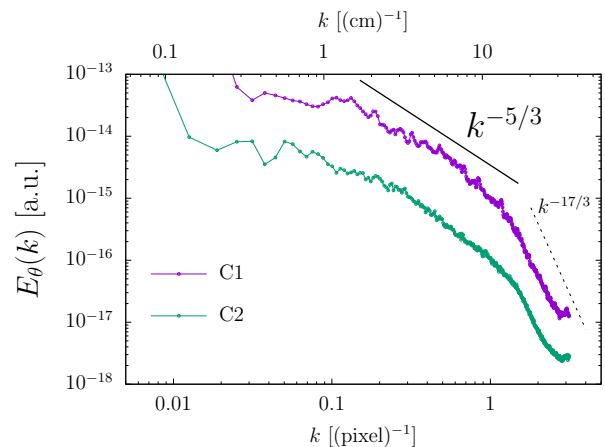


FIG. 4. Spectra of the luminance calculated in the two circular regions, C1 and C2, with the windowed Fourier transform. The solid line corresponds to the Obukhov–Corrsin spectrum,  $k^{-5/3}$ , in the inertial-convective range for the passive scalar advected by the homogeneous and isotropic turbulence. The dashed line corresponds to the Batchelor–Howells–Townsend spectrum,  $k^{-17/3}$ , in the inertial-diffusive range for the passive scalar turbulence. Here 1 [pixel] corresponds to 0.089 [cm].

to unit or low Schmidt number cases. However, the range  $k \geq 1 \text{ [(pixel)}^{-1}]$  is too narrow to conclude which one is more plausible. Furthermore, the smallest scales of the image can be more affected by the image compression or other procedures of the image processing. In this paper, we focus on the consistency with the OC spectrum.

In Fig. 4 we do not show the luminance spectrum in the small wavenumber range. That part of the spectrum is the Gaussian function, namely  $E_{\theta}(k) \propto \exp(-\sigma^2 k^2)$ , due to the windowing. The flat part of the luminance spectrum shown in Fig. 4 ends roughly at  $k = 2\pi/\sigma$  and the appearance of the power-law part in  $k > 2\pi/\sigma$  indicates that the  $k^{-5/3}$ -like power law reflects the nature of Kōrin’s flowing water motif. Given this consistency with the OC scaling law, we now address whether the intermittency corrections present, although the scaling range of the  $k^{-5/3}$ -like part of the spectrum in Fig. 4 is not more than a decade. We calculate the structure functions of the luminance in the next section.

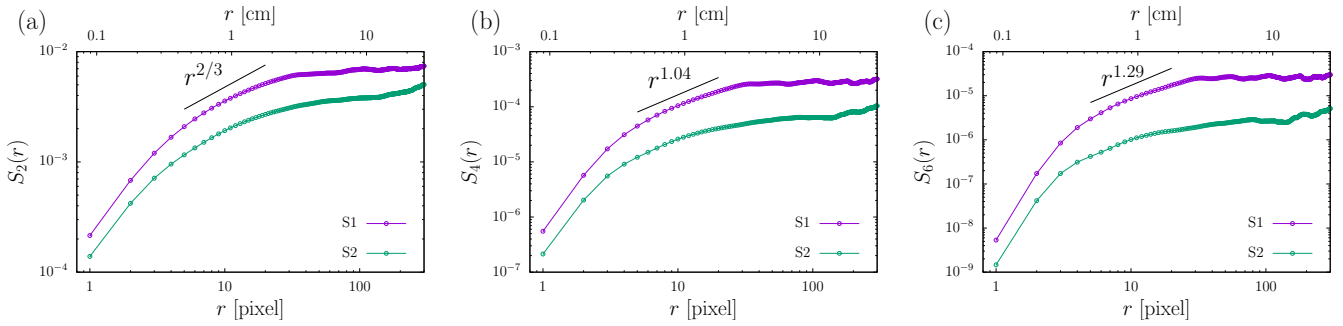


FIG. 5. Even-order structure functions,  $S_2(r)$  (a),  $S_4(r)$  (b), and  $S_6(r)$  (c), of the luminance calculated in the two square regions S1 and S2. The solid lines denote the power-law exponents of the structure functions of the passive scalar. The exponent  $2/3$  for the second-order one corresponds to the OC spectrum  $k^{-5/3}$ , for which the intermittency corrections are ignored. The values of the other exponents ( $1.04$  for  $p = 4$  and  $1.29$  for  $p = 6$ ) are taken from the numerical study of the passive scalar in the homogeneous and isotropic turbulence<sup>18</sup>, so that the intermittency corrections are present. As used in Fig. 4, one pixel corresponds to  $0.089$  cm.

#### IV. STRUCTURE FUNCTION

First we define the luminance increment as

$$\delta_r \theta = \theta(\mathbf{x} + \mathbf{r}) - \theta(\mathbf{x}). \quad (5)$$

Then the  $p$ -th order structure function of the luminance is defined by

$$S_p(r) = \langle \langle \delta_r \theta \rangle^p \rangle, \quad (6)$$

where  $\langle \cdot \rangle$  denotes a spatial average. Here we assume that the luminance is locally homogeneous and isotropic. Hence there is only  $r = |\mathbf{r}|$  on the left hand side of Eq. (6). We calculate the structure functions in the two square regions, S1 and S2, indicated in Fig. 2. The regions' coordinates are listed in Table II. The spatial average is taken with respect to  $\mathbf{x}$  in S1 or S2. The separation vector is set to either  $\mathbf{r} = (r, 0)$  or  $(0, r)$ . We take the averages over those two different directions of  $\mathbf{r}$  and over all the instances in which both points  $\mathbf{x}$  and  $\mathbf{x} + \mathbf{r}$  are within S1 or S2.

The structure functions for  $p = 2, 4$  and  $6$  calculated in this manner are shown in Fig. 5. We here focus on those even-order functions since they converge more quickly than odd-order ones. For the range of  $r$  where we expect a power-law scaling, let us go back to Fig. 4 in which the luminance spectrum is close to the OC scaling roughly in  $0.2 \leq k \leq 1$  (with the unit  $[(\text{pixel})^{-1}]$ ). This wavenumber range corresponds to  $6 \leq r \leq 30$  (with the unit  $[\text{pixel}]$ ).

In this range of  $r$ , the second-order structure function,  $S_2(r)$ , in Fig. 5(a) is roughly consistent with the OC scaling, which is now  $r^{2/3}$ . Let us recall that, if the OC scaling holds for the  $p$ -th order structure functions, the dimensional analysis yields  $S_p(r) \propto r^{p/3}$  (see, e.g., Ref. 19). Therefore  $S_2(r)$  confirms that the luminance follows roughly the OC scaling.

However, as shown in Fig. 5(b) and (c), the luminance structure functions for  $p = 2$  and  $4$  differ from  $r^{4/3}$  and  $r^2$ , respectively. Instead they are closer to  $r^{1.04}$  and  $r^{1.29}$ . Those values of the exponents<sup>18</sup> are so-called intermittent scaling exponents observed for the structure functions of the passive scalar advected in HIT. By intermittent<sup>22</sup> we mean that the

exponent of  $S_p(r)$  is different from  $p/3$  that is obtained by the dimensional argument<sup>13–15</sup> leading to the OC spectrum  $k^{-5/3}$ . It is known that, for the passive scalar turbulence, the power-law exponent for  $p = 2$  differs from  $2/3$  only slightly. However, for  $p > 2$ , the difference becomes larger, a phenomenon known as the intermittency<sup>16,17,19,22</sup>. Those differences, called intermittency corrections, are highlighted in the flatness  $S_4(r)/S_2^2(r)$  and the hyperflatness  $S_6(r)/S_2^3(r)$  of the luminance increment, as shown in Fig. 6. Variations are present depending on the regions, S1 and S2. But, overall, their  $r$ -dependence in the scaling range indicates that the intermittency of the luminance is approximately the same as the passive scalar advected by HIT.

Aiming at observing a cleaner power-law scaling, we use the SO(2) decomposition to extract the isotropic sector of  $S_p(r)$ <sup>23</sup>. However the isotropic sectors (not shown here) are basically the same as those shown in Fig. 5, indicating that the anisotropic effects are not strong. Therefore we consider that contamination making the graphs of  $S_p(r)$  in Fig. 5 not perfectly straight is primarily due to the inhomogeneity.

The intermittency of the structure functions can be a manifestation of the multifractality<sup>22</sup> of the luminance. It implies that the scale invariance of the luminance is broken. This can be observed in the probability distribution function (PDF) of the luminance increment for different  $r$ 's. We show the PDFs in the S1 and S2 regions in Fig. 7 for the normalized increment  $\widetilde{\delta_r \theta} = [\delta_r \theta - \langle \delta_r \theta \rangle] / [(\langle \delta_r \theta \rangle^2 - \langle \delta_r \theta \rangle^2)^{1/2}]$ . Obviously the PDFs are not Gaussian, having fat tails. More importantly, the normalized PDFs for several  $r$ 's in the scaling range are not collapsed to one master curve, although the differences between the PDFs are small. Thus the scale invariance being broken. This non-collapsed behavior of the non-Gaussian PDF is similar to that of the passive scalar in HIT<sup>17–19</sup>.

In summary, we find that Kōrin's flowing water motif respects approximately the physical law of the passive scalar advected by HIT. By the law, we mean not only the OC scaling of the second order quantities, but also the intermittent exponents of the fourth and sixth order structure functions. Those intermittent exponents of the passive scalar turbulence are known to be universal in the sense that they do not de-

TABLE II. Coordinates of the square regions, S1 and S2, for the structure functions. The centers are the same as those of C1 and C2 used in the windowed Fourier transform.

Region	Center [pixels]	Side length [pixels]
S1	(1650, 1175)	550
S2	(2515, 1275)	850

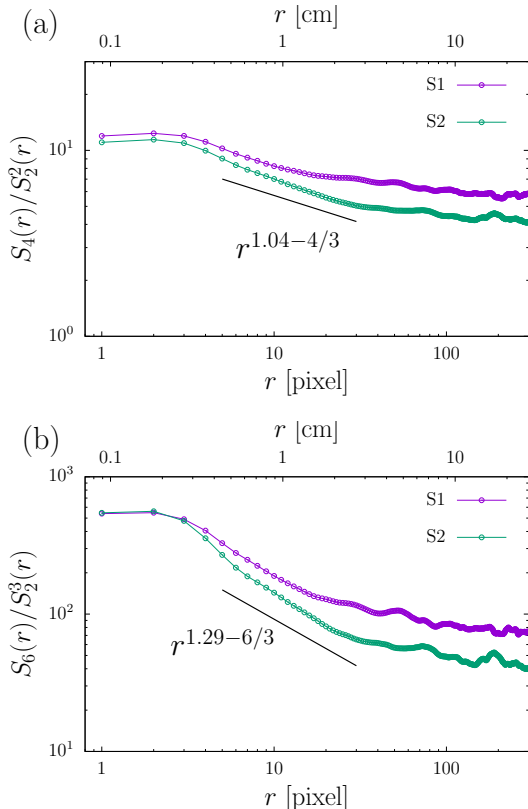


FIG. 6. Flatness  $S_4(r)/S_2^2(r)$  (a) and hyperflatness  $S_6(r)/S_2^3(r)$  (b) of the luminance increment as a function of  $r$ . The solid lines represent the power laws obtained from the scaling exponents indicated in Fig. 5.

pend on details of the system, such as how to inject the scalar quantity into the turbulent flow<sup>16,19</sup>. Such agreement for this highly stylized depiction of flow is likely not trivial at all and thus comes as a delightful surprise to us.

## V. CONCLUDING DISCUSSION

We have analyzed the luminance of the flowing river of *Red and White Plum Blossoms*. The spectrum of the luminance with the windowed Fourier transform followed closely  $k^{-5/3}$  in the two different regions of the river. This suggests that the luminance spectrum is consistent with the Obukhov–Corrsin spectrum of the passive scalar advected by HIT. We then calculate the even-order structure functions of the luminance up to the 6-th order and found that they showed the power-law behavior although its range was limited. The power-law expo-

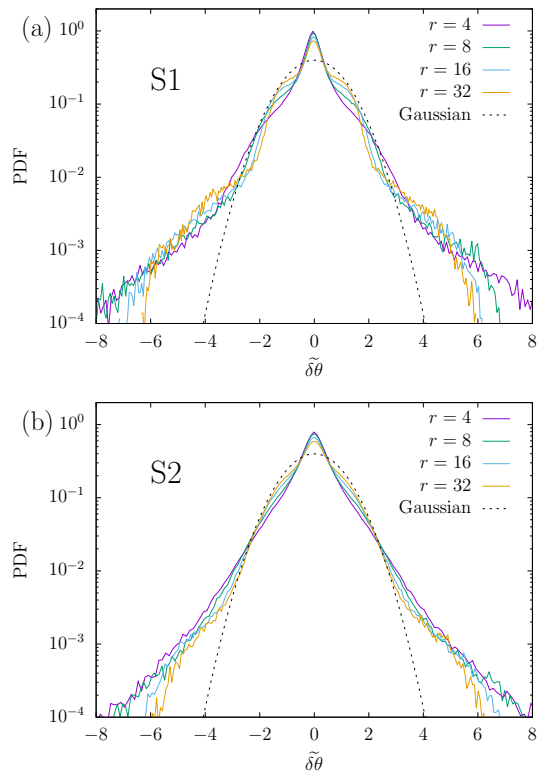


FIG. 7. Probability distribution functions of the luminance increments in the region S1 (a) and the region S2 (b) for several separation  $r$ 's in the scaling range of the structure functions. The values of  $r$ 's are given in pixels. The increment denoted by  $\tilde{\delta\theta}$  here is the normalized increment such that its mean and standard deviation are zero and unity, respectively.

nents of the luminance structure functions were also approximately consistent with the exponents with the intermittent exponents of the passive scalar in turbulence. Therefore we conclude that the flowing-water pattern of *Red and White Plum Blossoms* follows the universal (intermittent) scaling law of the passive scalar in the turbulent flow.

### A. Robustness of the scaling

Is the quantitative agreement between the stylized artwork and the natural phenomenon real or not? Of course, it can be just an artifact of the image processing, the photographic lighting or other factors, which are not related to the painting itself. To address this issue, we take two other JPG images of *Red and White Plum Blossoms*, which are supposedly independent from the one shown in Fig. 1. We analyze them in exactly the same manner.

One of the images is the one on the web site of the MOA museum of art<sup>24</sup> and the other one is on the Japanese Wikipedia on *Red and White Plum Blossoms*<sup>25</sup>. We call the former MOA image and the latter JAW image. We then call the image shown in Fig. 1 GAC image. The number of pixels of the MOA and JAW images are smaller than the GAC im-

age ( $1500 \times 658$  for the MOA image and  $2077 \times 925$  for the JAW image). Consequently, the scaling laws in the MOA and JAW images are less clear than what we observed in the GAC image. For the spectra in the regions equivalent to C1 and C2, the MOA and JAW images are consistent with the GAC image (here we take approximately the same regions for each image). For the structure functions in the region S1, the MOA image is not consistent with the GAC image, while the JAW image is consistent. In the region S2, only the 2nd-order structure functions of the MOA and JAW images are consistent with that of the GAC image. The 4th- and 6th-order structure functions in S2 of the MOA and JAW images are not consistent with that of the GAC image. The inconsistent structure functions are nearly  $r$ -independent except for the smallest few pixels, suggesting that the luminance have sharp spikes which are much higher than the background in the MOA and JAW images. Indeed, in the regions we observe the inconsistency, such spikes are found in the MOA and JAW images. The GAC image does not have comparable spikes.

This comparative little study indicates that the scaling property of the luminance is indeed affected by the image processing. However, if the luminance is sufficiently less spiky, or smooth enough, the scaling property seems to be robust. Of course, the number of pixels (resolution) is important for the smoothness, as the spectra of the MOA and JAW images in the region C2 do not have the hypothetical dissipation range, namely the part decreases faster than  $k^{-5/3}$ . Our conclusion here is that the less-spiky and high-resolution GAC image better reflects the nature of *Red and White Plum Blossoms* and that the turbulent scaling law we observed in the GAC image is likely robust.

## B. Why consistent?

The last question would be why and how Kōrin created the flowing water pattern, or *suiryu moyō* in Japanese, resulting in approximately the same intermittent scaling law of the passive scalar turbulence.

Now let us go back to *The Starry Night* that has the similar quantitative consistency with the real passive scalar turbulence<sup>9</sup>. In Ref. 9, it was argued that van Gogh’s very careful observation as a master of the post-impressionism led to the reproduction of the natural phenomenon. Furthermore the Batchelor scaling found in *The Starry Night* at the small scales was ascribed to the painting materials having a high Schmidt number<sup>9</sup>. For *The Great Wave off Kanagawa*, it was also concluded that Hokusai’s talent as an observer enabled him to capture and reproduce the physics of the waves<sup>5</sup>.

In the case of Kōrin, the same argument about his ability of observation applies without doubt. Regarding the materials used for *Red and White Plum Blossoms*, recent X-ray analyses<sup>26,27</sup> discovered that gold is not used in the foreground or background of the flowing river and that silver is used all over the river. But what was used precisely there is not identified yet. It may be of some future use to estimate the characteristic length of the small scales observed in this study. From the luminance spectrum shown in Fig. 4, the end of the  $k^{-5/3}$ -

like part is estimated as  $k \simeq 15 [(\text{cm})^{-1}]$ . It corresponds to 0.42 [cm], which can be regarded as the Kolmogorov dissipation length for the case of unit Schmidt number or the Obukhov–Corrsin length for the case of the low Schmidt number.

Regarding the technique of Kōrin used for the artwork, a recent study<sup>27</sup> involving present-day artists using similar materials argue that the flowing pattern is likely drawn freehand in one sitting and that use of a stencil could not explain the expressed sense of momentum (but use of a stencil is not completely ruled out). Paper marbling (*suminagashi* in Japanese) or water transfer printing is ruled out. Indeed, looking at Fig. 1 or enlarged photographs of various parts of the painting in Ref. 26, we can imagine that Kōrin drew without hesitation the lines of the flowing patterns. To have a feeling of the scale hierarchy Kōrin depicted, specifically in the panel number 98 on page 73 of Ref. 26, which corresponds to a part<sup>28</sup> of the region S2 in this paper, we observe that in that panel the scale ratio of the largest line width<sup>29</sup> to the smallest is about 85. This makes a good room to reproduce the broken self-similarity of the passive scalar turbulence.

Still the question remains: How did Kōrin then reproduce the intermittent scaling law in one sitting? Let us suppose that a creator of a stylized artwork discard many details of the object and picks up a few essential elements of it. Perhaps what Kōrin picked up from the complexity of the turbulent flow reflects what we now know as the universal scaling law of the passive scalar turbulence. Specifically his irregular hierarchy of the flow pattern ultimately ended up reproducing it. Further investigation of Kōrin’s construction of the flow may lead to a method that is in the same spirit of the recent mathematical construction of turbulent weak solutions to the Euler equations, known as the convex integration<sup>30</sup>. This may be a far-fetched idea. But, if it succeeds, then we see an example of the provocation made in Ref. 31: “Artists can complement scientific analysis and help in developing a comprehensive theory of turbulence”.

## ACKNOWLEDGMENTS

I thank the MOA Museum of Art, the Wikimedia Commons and the Google Art & Culture initiative for making the artwork available in the high-resolution JPG format. I gratefully acknowledge discussions with Kohei Okuyama. This work was supported by JSPS KAKENHI Grant Number JP19K03669 and Number JP23K03247.

## DATA AVAILABILITY STATEMENT

The JPG image of *Red and white plum blossoms*, which we analyzed here, is available at Wikimedia Commons, [https://commons.wikimedia.org/wiki/File:Ogata\\_Korin\\_-\\_RED\\_AND\\_WHITE\\_PLUM\\_BLOSSOMS\\_\(National\\_Treasure\)\\_-\\_Google\\_Art\\_Project.jpg](https://commons.wikimedia.org/wiki/File:Ogata_Korin_-_RED_AND_WHITE_PLUM_BLOSSOMS_(National_Treasure)_-_Google_Art_Project.jpg). The file was uploaded to Wikimedia Commons on November

26th, 2013 as written in the above web page. We retrieved the file on October 22nd, 2024 for the present analysis.

- <sup>1</sup>J. Monaghan and J. Kajtar, “Leonardo da Vinci’s turbulent tank in two dimensions,” *European Journal of Mechanics - B/Fluids* **44**, 1–9 (2014).
- <sup>2</sup>I. Marusic and S. Broomhall, “Leonardo da Vinci and Fluid Mechanics,” *Annual Review of Fluid Mechanics* **53**, 1–25 (2021).
- <sup>3</sup>A. Colagrossi, S. Marrone, P. Colagrossi, and D. Le Touzé, “Da Vinci’s observation of turbulence: A French-Italian study aiming at numerically reproducing the physics behind one of his drawings, 500 years later,” *Physics of Fluids* **33**, 115122 (2021).
- <sup>4</sup>J. H. Cartwright and H. Nakamura, “What kind of a wave is Hokusai’s *Great wave off Kanagawa* ?” *Notes and Records of the Royal Society* **63**, 119–135 (2009).
- <sup>5</sup>J. M. Dudley, V. Sarano, and F. Dias, “On Hokusai’s *Great wave off Kanagawa* : localization, linearity and a rogue wave in sub-Antarctic waters,” *Notes and Records of the Royal Society* **67**, 159–164 (2013).
- <sup>6</sup>J. L. Aragón, G. G. Naumis, M. Bai, M. Torres, and P. K. Maini, “Turbulent luminance in impassioned van Gogh paintings,” *Journal of Mathematical Imaging and Vision* **30**, 275–283 (2008).
- <sup>7</sup>J. Beattie and N. Kriel, “Is the starry night turbulent?” (2019), 10.48550/arXiv.1902.03381, arXiv:1902.03381 [physics].
- <sup>8</sup>W. H. Finlay, “The midrange wavenumber spectrum of van gogh’s starry night does not obey a turbulent inertial range scaling law,” *Journal of Turbulence* **21**, 34–38 (2020).
- <sup>9</sup>Y. Ma, W. Cheng, S. Huang, F. G. Schmitt, X. Lin, and Y. Huang, “Hidden turbulence in van Gogh’s *The Starry Night*,” *Physics of Fluids* **36**, 095140 (2024).
- <sup>10</sup>J. T. Carpenter, *Designing Nature: The Rinpa Aesthetic in Japanese Art* (Metropolitan Museum of Art, New York, 2012).
- <sup>11</sup>M. Yasui, “Katsushika Hokusai hitsu Kanagawaoki Namiura wo megutte (On *The Great wave off Kanagawa* by Katsushika Hokusai),” *Machikaneyama Ronsō, Bigaku hen*, Osaka University **30**, 49–70 (1996), in Japanese.
- <sup>12</sup>M. Fujisawa, “Katsushika Hokusai ga fugaku sanjyu rokkei ni miru Kōrin imēgi – ukiyoe to Rinpa (Images of Kōrin in Katsushika Hokusai’s *Thirty-six Views of Mount Fuji* – ukiyoe and Rinpa),” *Kokugakuin Zasshi, Kokugakuin University* **123-11**, 1–23 (2022), in Japanese.
- <sup>13</sup>A. Obukhov, “Structure of the temperature field in turbulent flows,” *Izvestiya Akademii Nauk SSSR, Seriya Geograficheskaya i Geofizicheskaya* **13**, 58–69 (1949).
- <sup>14</sup>S. Corrsin, “On the Spectrum of Isotropic Temperature Fluctuations in an Isotropic Turbulence,” *Journal of Applied Physics* **22**, 469–473 (1951).
- <sup>15</sup>H. Tennekes and J. L. Lumley, *A First Course in Turbulence* (MIT press, 1972).
- <sup>16</sup>G. Falkovich, K. Gawędzki, and M. Vergassola, “Particles and fields in fluid turbulence,” *Reviews of modern Physics* **73**, 913 (2001).
- <sup>17</sup>Z. Warhaft, “Passive scalars in turbulent flows,” *Annual Review of Fluid Mechanics* **32**, 203–240 (2000).
- <sup>18</sup>T. Watanabe and T. Gotoh, “Statistics of a passive scalar in homogeneous turbulence,” *New Journal of Physics* **6**, 40–40 (2004).
- <sup>19</sup>T. Gotoh and P. Yeung, “Passive scalar transport in turbulence: A computational perspective,” in *Ten Chapters in Turbulence*, edited by P. Davidson, Y. Kaneda, and K. R. Sreenivasan (Cambridge University Press, 2013) Chap. 3, pp. 87–131.
- <sup>20</sup>Recommendation Sector of International Telecommunication Union, *Recommendation ITU-R BT.709-6*, International Telecommunication Union (2015), [https://www.itu.int/dms\\_pubrec/itu-r/rec/bt/R-REC-BT.709-6-201506-I-1](https://www.itu.int/dms_pubrec/itu-r/rec/bt/R-REC-BT.709-6-201506-I-1)
- <sup>21</sup>G. K. Batchelor, I. D. Howells, and A. A. Townsend, “Small-scale variation of convected quantities like temperature in turbulent fluid part 2. the case of large conductivity,” *Journal of Fluid Mechanics* **5**, 134 (1959).
- <sup>22</sup>U. Frisch, *Turbulence* (Cambridge University Press, 1995).
- <sup>23</sup>L. Biferale and I. Procaccia, “Anisotropy in turbulent flows and in turbulent transport,” *Physics Reports* **414**, 43–164 (2005).
- <sup>24</sup>Retrieved on December 20th, 2024 from <https://www.moaart.or.jp/en/?collections=053>.
- <sup>25</sup>Retrieved on December 23th, 2024 from [https://commons.wikimedia.org/wiki/File:Ogata\\_K%C5%8Drin\\_-\\_Red\\_and\\_White\\_Plum\\_Blossoms](https://commons.wikimedia.org/wiki/File:Ogata_K%C5%8Drin_-_Red_and_White_Plum_Blossoms)
- <sup>26</sup>MOA Museum of Art and Tokyo National Research Institute for Cultural Properties (eds.) , *Kokuhou Kohakubaizu Byobue (National Treasure Red and White Plum Blossoms)* (Chuōkōron Bijutsu Shuppan, 2005) Mostly in Japanese but the main texts are also in English.
- <sup>27</sup>T. Uchida, S. Suzuda, S. Shimoyama, I. Nakai, H. Baba, K. Moriguchi, and K. Murase, “Kokuhou Kōrin hitsu Kouhakubaizu Byoubu no gihou zairyo ni kansuru kougakuteki kenkyu (Optical study on painting techniques and materials of National Treasure *Red and White Plum Blossoms* by Kōrin),” *Kajima Bijutsu Kenkyu Annual Report Supplement* **27**, 34–46 (2010) (the Kajima Foundation for the Arts, Tokyo, Japan) in Japanese.
- <sup>28</sup>It corresponds around the pixel coordinates (2420,975) in the image shown in Fig.1.
- <sup>29</sup>Those thickest and thinnest lines are distinct ones in the panel. It should be noticed also that the line width varies along one identical line.
- <sup>30</sup>T. Buckmaster, C. De Lellis, L. Székelyhidi Jr., and V. Vicol, “Onsager’s Conjecture for Admissible Weak Solutions,” *Communications on Pure and Applied Mathematics* **72**, 229–274 (2019).
- <sup>31</sup>Z. Warhaft, “The art of turbulence,” *American Scientist* **110**, 360 (2022).